

Terahertz waves generation in the cavity contains asymmetrical hyperbolic metamaterial

© O.N. Kozina,¹ L.A. Melnikov²

¹Saratov Branch, Kotelnikov Institute of Radio Engineering and Electronics, Russian Academy of Sciences, 410019 Saratov, Russia

²Yuri Gagarin State Technical University of Saratov, 410054 Saratov, Russia
e-mail: kozinaolga@yandex.ru

Received January 22, 2024

Revised January 22, 2024

Accepted January 22, 2024

Theoretical investigation of the terahertz waves propagation and generation in the cavity containing asymmetric hyperbolic metamaterial. The metamaterial under investigation is a nanoscale structure composed of periodically arranged layers of a semiconductor and inverted graphene. The aim of investigation is development of the component base for creating devices for terahertz generation and manipulation. The radiation characteristics in the cavity have been investigated by the transfer matrix method. The transformation of the electromagnetic field in a hyperbolic metamaterial, which is an anisotropic media, is described by Berreman matrix. A hyperbolic metamaterial is considered as a homogeneous medium with effective parameters due to the smallness of its period. Homogenization was carried out using the Maxwell–Garnett method. The conditions for efficient THz generation and the frequency range for THz generation are determined. The range of deviations of the tilt angle values of the optical axis of hyperbolic metamaterial for which the generation condition is satisfied and the effect of this angle variations on the generation frequency are determined. An estimation of the maximum allowable values of the asymmetrical hyperbolic metamaterial period have done. The saturation intensity of graphene amplification and the expected THz radiation field strength are calculated.

Keywords: graphene, nanostructure, frequency of generation, saturation.

DOI: 10.21883/0000000000

Introduction

Devices that allow operation at terahertz (THz) frequencies are promising for a wide range of applications — from safety systems and non-invasive treatment to time-domain spectroscopy [1,2]. Despite the success of research in this field of frequencies, the problem of creating a compact and efficient source of coherent THz radiation (THz laser) not solved. Various types of composite structures and their elements, including metamaterials are studied for creation of devices that can generate and process radiation in the THz frequency range [2–4]. It is known that metamaterials are artificially created periodic structures that have certain predetermined properties depending on their constituent materials and configuration [3–5]. The hyperbolic metamaterial (HMM), which is a special case of the so-called hyperbolic media (HM) is the most promising materials among the large number of metamaterials studied for creation of optical and THz radiation [6–7].

A hyperbolic medium is an anisotropic medium and is named due to the open type of dispersion dependencies in the space of wave vectors, which has the form of a hyperbola in cross section, unlike an ellipse for an ordinary medium [6]. A large number of slow waves with large values of the wave vector components are observed along the asymptotes of these hyperbolas, which means a high

density of photonic states inside the HM and results in an increased interaction of radiation with matter [5–8]. This property allows considering media and metamaterials with a hyperbolic type of dispersion as unique objects and motivates research on their application for the development of next-generation photonic devices. Only a small number of materials with a hyperbolic type of dispersion are known, for example, plasma in a strong electromagnetic field [6], graphite or boron nitride under certain difficult-to-achieve conditions [9]. Therefore, the designing and study of metamaterials supporting the hyperbolic type of dispersion is a relevant task.

A promising type of hyperbolic metamaterial for enhancing optical and THz radiation is a multilayer planar structure consisting of periodically ordered graphene layers in matrices of various types [8]. We are study HMM composed of nanometer layers of semiconductor and inverted graphene [5]. The use of graphene for creating HMM is based on its ability to support plasmon propagation [10,11]. In this case graphene is used as a constituent component of the metamaterial.

In this paper, we consider a special type of HMM — asymmetric hyperbolic metamaterial (AHMM) [5,12,13]. Asymmetry manifests itself as a difference in the properties of forward and reverse waves, while the transverse component of the wave vector remains fixed. Physically, the

asymmetry is realized by tilting the graphene layers relative to the outer boundaries of HM [5]. A large density of photonic states is created inside the structure when a plane wave falls on the AHMM with minimal reflection from the outer boundaries of the sample, which results in a high rate of spontaneous emission. It is important that photons with a high density of states excited in the AHMM can have an ideal bond with photons in free space due to the above asymmetry, which makes it possible to create conditions for the output of optical radiation accumulated in a hyperbolic medium to outer space. Such an AHMM has a significant gain in the THz frequency range [5]. The possibility of generating a THz wave in a single-mode in a resonator containing this AHMM is theoretically shown [13].

The propagation characteristics of THz radiation in a resonator containing AHMM are studied in this paper. The frequency range in which the conditions for effective generation of THz radiation are maintained is determined, as well as the impact of the geometric parameters of the AHMM on the predicted frequency of THz generation. The eigenvalues of the transmission matrix of the full resonator bypass for forward and reverse waves are studied for this purpose in this paper. The imaginary part of the eigenvalues corresponds to an unsaturated gain. The real part determines the frequency of laser oscillations. The effect of saturation gain in graphene is investigated and the predicted power of THz radiation is estimated. To calculate the output power of the laser, the saturation intensity of the laser junction, the unsaturated gain, loss and transmission of the output mirror are determined. The dependence of the chemical potential of graphene on the intensity of the electric field transverse to graphene sheets was studied for evaluation of the saturation intensity. A change in the chemical potential (Fermi energy) entails a change in amplification due to the interband inversion of populations. A numerical estimate of graphene saturation intensity and the expected value of THz radiation power is provided.

The assessment of the limits of variation of the values of the geometric parameters of the AHMM, under which the THz generation conditions are met is an important aspect in the study of these structures. This is of great importance for creating a real sample due to the small size of the structure. The effect of the change of the angle of inclination of the optical axis relative to the external boundaries of the AHMM is studied for a comprehensive assessment of the possibility of maintaining an effective THz generation mode. The range of possible deviations of the values of the angle of inclination of the optical axis of the AHMM from the optimal one and the effect of this deviation on the change in the generation frequency is determined in this paper. The maximum permissible values of the AHMM period was estimated to determine the frequency range of THz generation. It is shown that the studied structure is unique in terms of the variability of its parameters to achieve wave generation in the THz frequency range. The results obtained are of great importance both for the construction of a rigorous theory of THz generation,

taking into account the effect of saturation amplification, and for the practical implementation of THz generation in graphene-based structures and metamaterials.

1. Model and characteristics of the resonator and HMM

A resonator with reflective walls, in which an asymmetric hyperbolic material (AHMM) is located is considered in this paper. The resonator (Fig. 1) consists of isotropic regions indicated by the numbers 1 and 2 (length l_1 and l_2), characterized by losses (the total width of the isotropic region $l = l_1 + l_2$), and AHMM thick h (the area indicated by the number 3). The complete bypass of the resonator is characterized by a length of one period $L = l + h$. The reflecting walls of the resonator — the outer planes are purple in color, arranged horizontally.

The AHMM is a multilayer structure consisting of periodically alternating layers of inverted graphene (red planes) and a semiconductor located at an angle relative to the boundaries of the AHMM layer, the region 3 in Fig. 1. The asymmetry occurs due to tilting of the optical axis (angle θ) relative to the boundaries of the AHMM layer. The forward and reverse waves propagating in the structure acquire different properties due to this tilting while maintaining the components of the wave vector. As a result, conditions are created for the output of THz radiation generated in a hyperbolic medium into outer space.

HMMs are highly anisotropic uniaxial media. In this case, the properties of the medium are described by the dielec-

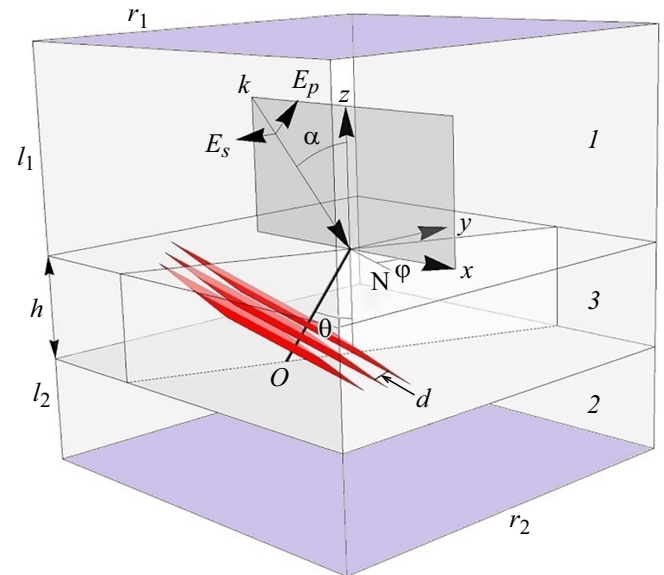


Figure 1. Schematic representation of a complex resonator containing an AHMM. The oblique red planes inside the AHMM (area 3) symbolize graphene layers. O — optical axis, θ — angle between the optical axis and the axis z (angle of inclination of the optical axis), N — node line, φ — angle between the axis x and the node line, α — angle of incidence of radiation on the structure, gray surface — plane of incidence, h — total thickness of AHMM.

tric constant tensor $\varepsilon = \{\{\varepsilon_{\perp}, 0, 0\}, \{0, \varepsilon_{\perp}, 0\}, \{0, 0, \varepsilon_{\parallel}\}\}$. The main values of the dielectric constant tensor ε_{\parallel} and ε_{\perp} have different signs [6–8].

The characteristics of the hyperbolic layer can be described using the homogenization method because of the small size of the AHMM period compared to the length of the waves propagating in it. In this case, the composite structure is considered as an effective medium with averaged parameters [5,12,14]. An exact method for solving the dispersion equation for a periodic structure using the Floquet-Bloch theorem and the homogenization method based on the Maxwell–Garnett model, and a complete coincidence of the results for the considered AHMM is shown in Ref. [12]. The dielectric constant of the effective medium is calculated using the formula

$$\varepsilon_{\perp} = \varepsilon_{\parallel} + \frac{i}{d\omega\varepsilon_0}[\sigma'(\omega, E_0) + i\sigma''(\omega, E_0)],$$

where $\varepsilon_{\parallel} = \varepsilon_h$ —the dielectric constant of the material in which the graphene layers are located, ω — angular frequency, $\sigma(\omega, E_0)$ — the surface conductivity of graphene, E_0 — transverse (relative to the plane of graphene sheets) component of the electric field strength vector, ε_0 — electric constant, d — period AHMM.

Graphene is described in terms of the surface conductivity of inverted graphene $\sigma(\omega, E_0) = (\sigma_{\text{intra}} + \sigma_{\text{inter}})$, which depends on the frequency and component of the electric field vector transverse to the graphene plane. The change of E_0 affects the value of the chemical potential μ_c . This approach provides a possibility to conduct a comprehensive analysis of the THz wave generation process in AHMM, taking into account the saturation effect of graphene amplification. The Kubo formula (formula (2) from Ref. [15]) was used to calculate the conductivity of graphene layers. Calculations were carried out for AHMM, in which silicon carbide was selected as a material alternating with graphene layers. The choice of this type was motivated by the results of experimental work, which describes attempts to grow graphene layers on a silicon carbide substrate [16]. The data from Ref. [17] are used in calculations of the dielectric function of silicon carbide, where all possible SiC polytypes are described and some experimental and theoretical values of the dielectric function are presented. Moreover, a high agreement between the average values of experimental data and theoretical ones was shown in Ref. [18]. The calculation of the dependence of ε_{\perp} on frequency when using the dielectric function of silicon carbide, taking into account polytypicity, is described in Ref. [5]. In the theory presented, this type of semiconductor can be replaced by another one using the corresponding dielectric function of the semiconductor.

2. Method

The creation of conditions for the THz wave generation in the AHMM of the considered type is based on an

abnormally high density of electromagnetic states along the asymptotes of hyperbolic frequencies, which leads to a high rate of spontaneous emission and to the emergence of a large number of ordinary and extraordinary modes propagating in the forward and reverse directions inside the structure. The characteristics of these waves were studied using a rigorous mathematical approach using the transmission matrix method. The field transformations inside the AHMM are described by the Berreman matrix [19], which allows calculating the optical characteristics of forward and reverse waves at an arbitrary radiation angle, taking into account the anisotropy of the medium. The method allows calculating the eigenvalues of the final matrix of the complete resonator bypass, the amplitude of the components of the electric and magnetic fields and the magnitude of the Poynting vector.

The characteristics of the radiation propagating in the resonator can be obtained from the product of the transmission matrices for the resonator medium $P_0(l_1)$ and $P_0(l_2)$ and the hyperbolic layer $P(h)$: $P_t = P_0(l_1)P(h)P_0(l_2)$. Maxwell's equations in differential matrix form are used for considering a medium with continuously changing parameters. The following matrix expression is valid to describe the linear transformation between the four tangential components of the electric and magnetic fields at the input and output of an anisotropic optical system [19–21]:

$$\frac{\partial}{\partial z}\Psi = \frac{i\omega}{c}\Lambda\Psi.$$

Ψ is a column vector containing, in general, all tangential components of the electric and magnetic fields in this expression. In our case, the column vector Ψ has the form:

$$\Psi = \begin{pmatrix} E_x \\ H_y \\ E_y \\ -H_x \end{pmatrix}.$$

The elements of the matrix Λ are defined by expressions containing the components of the wave vector, the components of the dielectric constant tensor of the effective medium and the Euler angles θ , φ , ψ [19–21]. All calculations are performed under the assumption $\psi = 0$.

When considering active media with gain or loss, the components of the dielectric constant tensor ε_{\perp} and ε_{\parallel} have complex values. The electromagnetic fields of incident, reflected and transmitted waves are related by the following ratio for a medium with a thickness of h

$$\Psi_T = P(h)(\Psi_I + \Psi_R),$$

where Ψ_T , Ψ_I and Ψ_R —column vectors of the transmitted, incident and reflected waves, which are expressed as follows:

$$\Psi_T = \begin{pmatrix} T_x \\ \frac{1}{\cos\alpha}T_x \\ T_y \\ \cos\alpha T_{y,x} \end{pmatrix},$$

$$\Psi_R = \begin{pmatrix} R_x \\ -\frac{1}{\cos \alpha} R_x \\ R_y \\ -\cos \alpha R_y \end{pmatrix}. \quad (1)$$

The matrix $P(h)$ can be calculated using the formula

$$P(h) = \exp(i\omega h \Delta / c) \equiv \sum_{k=1}^4 (\exp(i\omega h \Lambda_k / c) \times (\prod_{i \neq k} (\Delta - \Lambda_i I) / \prod_{i \neq k} (\Lambda_k - \Lambda_i)))$$

Λ_{ik} — the eigenvalues of the matrix Δ , I — the unit matrix.

The eigenvalues κ_i of the final matrix P_t are derived from the formula $\Lambda_i = \exp(i\kappa_i L)$ and allow us to determine the values of the gain of the studied structure and the frequency of THz wave generation. The frequency of the generated THz wave f is determined by the values k_z , for which the condition $\text{Re}(\kappa_i L) = 2\pi m$, $m = 0, \pm 1, \pm 2, \dots$ is fulfilled. The imaginary part of the eigenvalue $\text{Im}(\kappa_i)$ characterizes the gain in the structure. Hence, the frequency of the mode and the intensity of the mode are solutions to the equations

$$\text{Re}[\chi_i(k_z, E_0) = 0], \quad \text{Im}[\chi_i(k_z, E_0) = 0]. \quad (2)$$

3. Results

Based on the described approach, the characteristics of the radiation propagating in the resonator are studied. The forward and reverse ordinary and extraordinary waves with their corresponding eigenvalues of the transmission matrix propagate in the resonator to completely bypass the resonator owing to the use of AHMM as an active medium. Graphs of the dependence of the eigenvalues of the resonator transmission matrix on frequency allow determining the fulfillment of the condition (2).

Previously, using the dependence σ and ε_{\perp} on k_z we determined that the range from 2 to 12 THz has the potential to generate THz radiation in the considered AHMM at the Fermi energy value $E_F = 25$ MeV [5]. The following conditions are met in this frequency range: $\text{Re}(\sigma) < 0$ — corresponds to the presence of gain in graphene; the considered AHMM has hyperbolic properties $\text{Re}(\varepsilon_{\perp}) < 0$ and gain $\text{Im}(\varepsilon_{\perp}) < 0$ simultaneously [5].

The dependences of the eigenvalues of the resonator transmission matrix on frequency have been studied throughout this range [13]. Based on a comprehensive analysis of the eigenvalues of the transmission matrix of the complete resonator bypass, including an estimate of the values of the imaginary part of the eigenvalues and the fulfillment of condition (2), it is determined that stable values of the gain factor and the fulfillment of the THz generation condition are fulfilled only in part of the above range, namely from 2.9 to 4.7 THz, which corresponds to the interval $0.06 < k_z < 0.095 \mu\text{m}^{-1}$. The choice of a narrower part of the frequency range to create THz generation

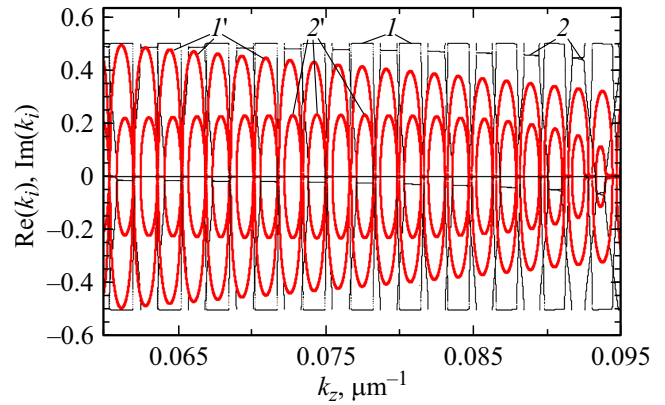


Figure 2. Real (black curves) and imaginary (red curves) parts of the eigenvalues κ_i matrices P_t depending on k_z . Lines 1 — $\text{Re}(\kappa_i)$ for ordinary modes, 2 — $\text{Re}(\kappa_i)$ for extraordinary modes. Lines 1' — $\text{Im}(\kappa_i)$ for ordinary modes, 2' — $\text{Im}(\kappa_i)$ for extraordinary modes. Calculation parameters: $L = 1320 \mu\text{m}$, $h = 5 \mu\text{m}$, $d = 50 \text{ nm}$; $\theta = 55^\circ$, $\varphi = \pi/2$, $\alpha = 15^\circ$; $E_F = 25 \text{ meV}$, $T = 300 \text{ K}$, $t = 10^{-12} \text{ s}$. Frequency range $2.9 < f < 4.7 \text{ THz}$ ($0.06 < k_z < 0.095 \mu\text{m}^{-1}$).

is associated with the values $\text{Im}(\kappa_i)$, which characterize the gain. It is shown in Ref. [13] that the gain reaches the values necessary for generation only in the selected frequency range (2.9–4.7 THz). The spectral dependences of the real and imaginary parts of the logarithms of eigenvalues determine ordinary and extraordinary (forward and reverse) eigenwaves in the resonator (Fig. 2).

The red lines correspond to the imaginary part of the eigenvalues, the black lines correspond to the real part of the eigenvalues. The curves 1 ($\text{Re}(\kappa_i)$) and 1' ($\text{Im}(\kappa_i)$) correspond to ordinary waves, curves 2 ($\text{Re}(\kappa_i)$) and 2' ($\text{Im}(\kappa_i)$) correspond to extraordinary waves. It is possible to notice based on the value of the imaginary part κ_i that ordinary modes have a greater gain than extraordinary modes. The occurrence of a large number of extraordinary modes in the resonator causes the generation of THz radiation.

The orientation of the optical axis of the HM is a key factor for the output of a large number of extraordinary modes to the external space. The angle of inclination of the layers is determined by analogy with the Brewster angle. Comparing the set of wave types propagating in the considered resonator with the AHMM with the set of types for a resonator containing a similar symmetrical metamaterial without inclination of the AHMM layers relative to its outer boundary ($\theta = 0$), while maintaining all other parameters, it can be stated that there are no extraordinary modes in the latter case. Graphs for a symmetrical sample are not provided for saving the space.

A fragment of the graph of the dependence of the real and imaginary parts of the eigenvalues of the transmission matrix from k_z on a large scale for a narrow frequency range $4.113 < f < 4.133 \text{ THz}$ ($0.0822 < k_z < 0.08362 \mu\text{m}^{-1}$) is presented to demonstrate the fulfillment of condition (2)

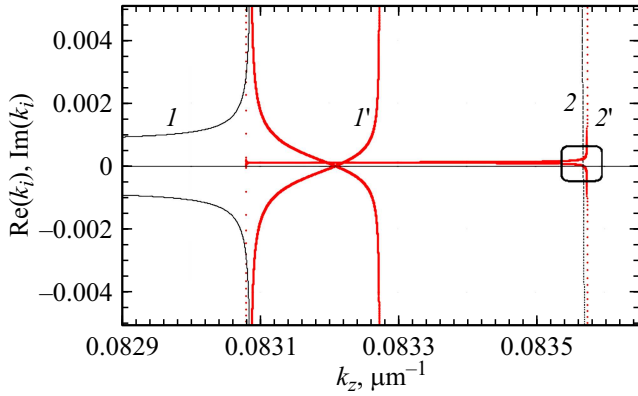


Figure 3. Real (black curves) and imaginary (red curves) parts of the eigenvalues κ_i of the matrix Pt depending on k_z . Lines 1 — $\text{Re}(\kappa_i)$ for ordinary modes, 2 — $\text{Re}(\kappa_i)$ for extraordinary modes. Lines 1' — $\text{Im}(\kappa_i)$ for ordinary modes, 2' — $\text{Im}(\kappa_i)$ for extraordinary modes. Calculation parameters: $L = 1320 \mu\text{m}$, $h = 5 \mu\text{m}$, $d = 50 \text{ nm}$; $\theta = 55^\circ$, $\varphi = \pi/2$, $\alpha = 15^\circ$; $E_F = 25 \text{ meV}$, $T = 300 \text{ K}$, $t = 10^{-12} \text{ s}$. Frequency range $4.113 < f < 4.133 \text{ THz}$ ($0.0822 < k_z < 0.08362 \mu\text{m}^{-1}$).

(Fig. 3). It can be seen that the condition (2) is satisfied for the extraordinary mode (indicated by a square), while for the ordinary mode $\text{Re}(\kappa_i) \neq 0$.

It is possible to conclude after considering each frequency value at which transitions of the eigenvalue curves of the full resonator bypass matrix through zero are observed that the presence of a large number of ordinary modes with large gain values is not sufficient to generate stable generation of THz waves. The slope of the layers makes it possible to create conditions for the effective output of radiation with a high density of photonic states accumulated in a hyperbolic medium into the cavity space, which manifests itself as the occurrence of a large number of unusual modes. It was determined according to preliminary estimates, based on numerical modeling, that the generation bandwidth is $\Delta f \approx 0.00455 \text{ THz}$ [13].

4. The effect of the deviation of the angle of inclination of the optical axis on the generation frequency

An important aspect in studying the prospects of these structures is the assessment of the limits of changes in the geometric parameters of the AHMM, under which the conditions for THz generation are met. Since the orientation of the optical axis is one of the main factors, we will study the effect of the deviation of the angle of inclination of the optical axis θ from the optimal one on the gain and fulfillment of the mode generation condition.

The calculated optimal value of the angle of inclination of the optical axis is $\theta = 55^\circ$. Fig. 4 shows the dependences of $\text{Re}(\kappa_i)$ and $\text{Im}(\kappa_i)$ of one extraordinary mode on k_z for three values of the angle of inclination of the optical axis 50°

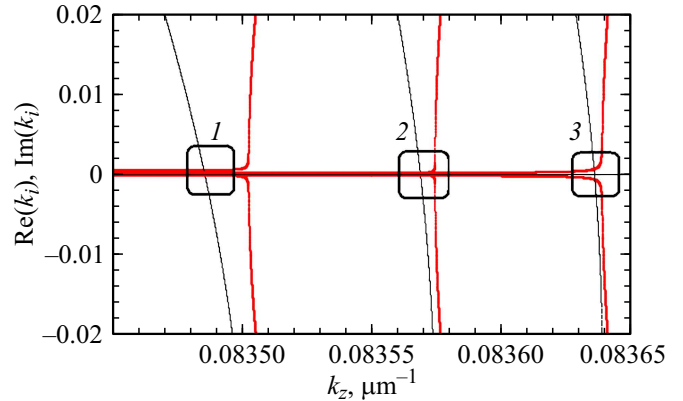


Figure 4. Demonstration of the fulfillment of the condition (2). The real (black curves) and imaginary (red curves) parts of the eigenvalues of the matrix P_i depending on k_z for an extraordinary wave at three values of the angle of inclination of the optical axis: 1 — $\theta = 50^\circ$, 2 — 55° , 3 — 60° : Calculation parameters: $L = 1320 \mu\text{m}$, $h = 5 \mu\text{m}$, $d = 50 \text{ nm}$; $\varphi = \pi/2$, $\alpha = 15^\circ$; $E_F = 25 \text{ meV}$, $T = 300 \text{ K}$, $\tau = 10^{-12} \text{ s}$.

(indicated by a digit 1), 55° (2) and 60° (3). The fulfillment of condition (2) is observed for all three considered values of the angle θ , the intersections $\text{Re}(\kappa_i)$ with the axis x are highlighted by squares. The values of the resonant frequency at different θ differ only in the fourth decimal place and correspond to the generation frequency $f \approx 4.13 \text{ THz}$. The condition of THz generation is violated (2) with values θ less than 50° and more than 60° . Therefore, when the angle of inclination of the optical axis changes within $\pm 5^\circ$, the THz waves generation in A resonator containing an asymmetric hyperbolic layer is maintained and implemented in the selected frequency range.

5. Impact of the magnitude of the structure period on the THz generation frequency range

An important issue is the evaluation of the impact of the period value of the AGMM structure d on the change of the frequency range in which THz wave generation is predicted. This range is determined primarily by the conductivity of graphene and the effective dielectric constant of the hyperbolic structure [5]. The correspondence of the previously selected optimal value of the AHMM period to the frequency range 2.9 to 4.7 THz defined here, in which the generation condition is fulfilled, is evaluated in this paper. For this purpose, the dependence of the effective dielectric constant of the AHMM on the frequency at 10 different values of the period d is considered. The result is shown in Fig. 5. Solid curves correspond to $\text{Re}(\varepsilon_\perp)$, dashed curves correspond to $\text{Im}(\varepsilon_\perp)$. The generation frequency range corresponds to frequencies at which the AHMM has hyperbolic properties ($\text{Re}(\varepsilon_\perp) < 0$) and amplification properties ($\text{Im}(\varepsilon_\perp) < 0$) simultaneously.

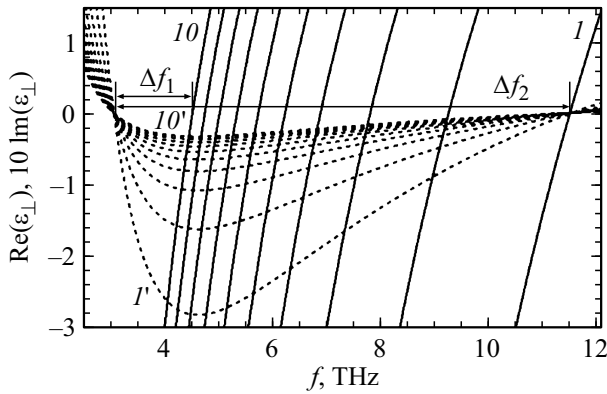


Figure 5. The real and imaginary parts of the effective permittivity of the AHMM as a function of frequency. Solid curves correspond to $\text{Re}(\varepsilon_{\perp})$, dashed curves correspond to $\text{Im}(\varepsilon_{\perp})$. For 10 values of the AHMM period from $d = 10$ nm (curves 1 and 1') to 100 nm (curves 10 and 10'), in increments of 10 nm. $E_F = 25$ meV, $T = 300$ K, $t = 10^{-12}$ s.

The values of the AHMM period d varied from 10 nm (curves 1 and 1') to 100 nm (curves 10 and 10'), in increments of 10 nm (Fig. 5). The chart clearly shows that the frequency range Δf in which THz wave generation is possible, decreases with an increase of the period of the structure. Namely, the frequency range Δf is from 3 to 4.8 THz for $d = 100$ nm. The interval Δf increases with a decrease of the period and it ranges from 2.25 to 11.25 THz for the value of the period AHMM $d = 10$ nm. However, as we noted above, the gain factor acquires values sufficient to generate a THz wave only in the frequency range from 2.9 to 4.7 THz. Fig. 5 shows that this range is maintained at values d from 50 to 100 nm. Therefore, it is impractical to choose an AHMM period less than 50 nm. The variation of the AHMM period from 50 to 100 nm changes the value of the THz generation frequency only in the fourth decimal place [13].

The described method allows determining the optimal AHMM period and the limits of possible changes in its values, at which the generation of a THz wave occurs in the selected frequency range. This fact is important both for theoretical calculations and for experimental sample production. The miniaturization of devices is often associated with insufficient accuracy of compliance with specified geometric parameters, especially at nanometer scales. The method used here will allow synchronizing the choice of resonator and AHMM parameters to achieve THz wave generation in a certain frequency range.

6. Consideration of the saturation effect of gain in graphene

The propagation of THz waves was studied in the resonator taking into account the effect of saturation gain in graphene. The value of the chemical potential of graphene sheets μ_c depends on the component of the electric field of

THz radiation E_0 [22] transverse to the graphene plane. The THz radiation itself may have such a field component, which will result in the saturation. The field of THz radiation generated in this AHMM owing to the amplification inside the system acts in this study as a field affecting the system and changing the value of the chemical potential of graphene. Starting with small values E_0 corresponding to thermal fluctuations in the resonator, it is possible to calculate the change of E_0 using the iteration method, and, consequently, μ_c , and the corresponding eigenvalues of the matrix P_t , which allows determining the frequency of mode generation using the equation $\text{Re}[\kappa_i(k_z, E_0)] = 0$. The change of E_0 results in a slight change of the value of k_z and to a more pronounced change of $\text{Im}(\kappa_i)$, which determines the gain. Therefore, E_0 changes until the condition $\text{Im}[\kappa_i(k_z, E_0)] = 0$ is met.

The relationship between the chemical potential of graphene μ_c and the transverse component of the electric field of THz radiation E_0 is expressed by the formula [22]

$$E_0 = \left[\frac{e}{\pi \hbar^2 v_F^2 \varepsilon_b} \right] \int_0^{\infty} d\varepsilon (f_d(\varepsilon) - f_d(\varepsilon + 2\mu_c)),$$

where $f_d(\varepsilon)$ — Fermi-Dirac function, ε_b — dielectric constant of graphene. The function $f_d(\varepsilon)$ is defined by the formula $f_d(\varepsilon) = 1/(\exp[(\varepsilon - \mu_c)/(k_B T)] + 1)$. The dependence of the chemical potential of graphene sheets μ_c on the transverse component of the electric field of THz radiation E_0 is shown in Fig. 6.

The value of the component of the electric field strength vector E_0 transverse to the graphene plane, which corresponds to the saturation of graphene gain, was estimated using Beer–Lambert law. The initial value of the gain is determined from graphs of the dependence of the eigenvalues of the Berreman matrix on z -components of the wave vector k_z and is $\text{Im}(\kappa_i) \approx 0.25$ (Fig. 2). The losses are set by the values of the reflection coefficients of mirrors at the boundaries of the resonator r_1 and r_2 . The time of relaxation of charge carriers in graphene $\tau = 10^{-12}$ s. As a result of calculations, it was found that saturation of

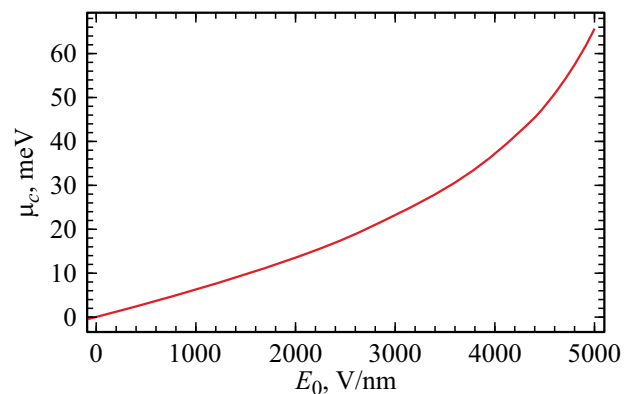


Figure 6. Dependence of the chemical potential μ_c on the transverse component of the electric field E_0 .

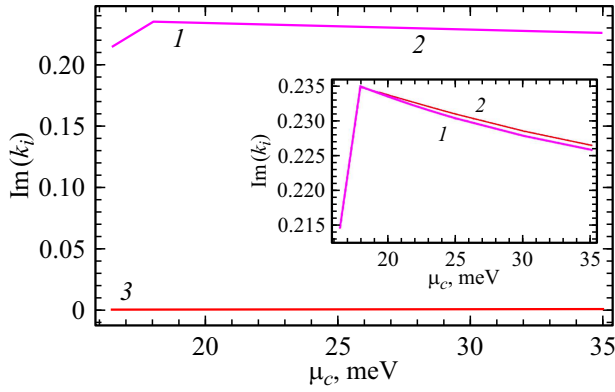


Figure 7. Dependence of the gain on the values of the chemical potential in graphene μ_c [MeV] for extraordinary modes: curve 1 (straight wave) — $\text{Im}(\kappa_1)$, 2 (reverse wave) — $\text{Im}(\kappa_2)$. The line 3 characterizes the loss level (0.0009). The insert shows the difference between forward (1) and reverse (2) extraordinary waves on a large scale.

gain in graphene occurs when the electric field strength is higher than the value $E_0 = 2.7 \cdot 10^{12}$ V/m. The value of the chemical potential corresponding to the balance of losses and saturated gain, $\mu_c = 19.5$ MeV is determined using the graph of the dependence of the chemical potential μ_c on E_0 (Fig. 6).

The dependence of the unsaturated gain on the chemical potential of graphene sheets for unusual waves at the frequency $f = 4.13$ THz is shown in Fig. 7. The red line 3 characterizes the level of losses. The magenta lines correspond to the straight (curve 1) and reverse (curve 2) extraordinary waves. It can be seen that the gain in the studied resonator significantly exceeds the loss level due to the presence of AHMM of this type due to the excitation of a large number of unusual modes in a hyperbolic medium. The curves related to the forward and reverse extraordinary waves show slightly different amplification due to the asymmetry of the metamaterial. Figure 7 shows the same dependence with a smaller step on the ordinate scale to demonstrate this effect.

Assuming that the relaxation time of the charge carrier pulse in graphene is equal to 10^{-12} s, it is possible to conclude that the saturation of the gain occurs proportionally to the electric THz field strength averaged in this time interval. The calculated value of the intensity of THz radiation to achieve the effect of saturation gain is about $1.2 \cdot 10^{15}$ W/m² for the frequency 3–4 THz.

The z -component of the Poynting vector $P_z = E_x H_y^* - E_y H_x^*$ is calculated for estimating the expected power:

$$P_z = E_x E_y^* - E_y E_x^*.$$

The spatial components of the electric field are found from the equation

$$k_z E_z + k_x E_x + k_y E_y = 0.$$

The equation for finding E_z is as follows with the condition $k_y = 0$ [5] selected at the initial stage of the study:

$$E_0 = E_x \sin \vartheta + E_z \cos \vartheta.$$

The components E_x and E_y are found from the expressions of the column vectors of the incident and reflected waves Ψ_I and Ψ_R , formula (5). It was found based on the analysis of the dependence of the components of the Poynting vector on k_z that at frequencies corresponding to the amplification, the energy flow in the resonator increases.

The expected power of the electric field of THz radiation, at the above value of the intensity of THz radiation corresponding to the saturation of the gain, is in the order of $3.5 \cdot 10^3$ V/nm. Certainly, this value is quite significant, but it should be noted that the cross-section of the THz radiation beam is quite small and is determined by the radius of the graphene optical pumping laser beam, therefore the total power of THz radiation may be relatively small. The high value of the saturation intensity of the gain means that significant THz radiation power can be expected in this structure when using the optimal transmission of the output mirror. It is also necessary to include the pumping process in this theory for a more detailed analysis of the action of the THz laser, which will be done in subsequent studies. In the framework of this work, pumping is described as a change in the chemical potential of graphene.

Conclusion

The process of propagation and generation of THz radiation in a resonator containing an AHMM consisting of thin periodically ordered layers of semiconductor and inverted graphene is theoretically investigated. The possibility of THz generation in the considered structure is demonstrated, taking into account the effect of saturation gain. THz generation conditions are defined. An increase of gain owing to the presence of this type of AHMM is shown. The frequency range in which THz generation occurs is determined. The value of the electric field of the THz wave, at which the gain saturation occurs, is calculated and the possible power of THz radiation is estimated. The range of deviations of the angle of inclination of the optical axis of the AHMM from the optimal one, for which the THz generation condition is fulfilled, and the effect of variations of this angle on the change in the generation frequency are determined. It is established that a change of the angle of inclination of the optical axis within the range of $\pm 5^\circ$ does not significantly affect the process of generation of THz waves in the considered resonator and the value of the generation frequency. The maximum permissible values of the AHMM period were estimated. Taking into account the impact of the deviation of the geometric parameters of the resonator and the AHMM from geometric parameters optimally selected for achieving effective generation of THz waves is extremely important because of the challenges of

manufacturing ultra-small structures. The results obtained can be used to create graphene-based THz radiation sources.

Funding

The study has been performed under the state assignment.

Conflict of interest

The authors declare that they have no conflict of interest.

References

- [1] X.-C. Zhang, J. Xu. *Introduction to THz Wave Photonics* (Springer-Verlag, NY., 2009)
- [2] A. Khalatpour, A.K. Paulsen, Ch. Deimert, Z.R. Wasilewski, Q. Hu. *Nature Photonics*, **15** (1), 16 (2012). DOI: 10.1038/s41566-020-00707-5
- [3] I. Smolyaninov, V.N. Smolyaninova. *Solid-State Electron.*, **136**, 102 (2017). DOI: 10.1016/j.sse.2017.06.022
- [4] T. Guo, L. Zhu, P.-Y. Chen, C. Argyropoulos. *Opt. Mater. Express*, **8**, 3941 (2018). DOI: 10.1364/OME.8.003941
- [5] O.N. Kozina, L.A. Melnikov. *Izvestiya Saratovskogo universiteta. Novaya seriya. Seriya: Fizika*, **19** (2), 122 (2019) (in Russian). DOI: 10.18500/1817-3020-2019-19-2-122-131
- [6] F.I. Fedorov. *Optika anizotropnyh sred* (Academy of Sciences of the BSSR, Minsk, 1958)
- [7] L. Felsen, N. Marcuvitz. *Radiation and Scattering of Waves* (Englewood Cliffs, NJ.: Prentice-Hall, USA, 1973)
- [8] V. Iorsh, I.S. Mukhin, I.V. Shadrivov, P.A. Belov, Y.S. Kivshar. *Phys. Rev. B*, **87**, 075416 (2013). DOI: 10.1103/PhysRevB.87.075416
- [9] J. Sun, J. Zhou, B. Li, F. Kang. *Appl. Phys. Lett.*, **98** (10), 101901 (2011). DOI: 10.1063/1.3562033
- [10] D. Yadav, G. Tamamushi, T. Watanabe, J. Mitsushio, Y. Tobah, K. Sugawara, A.A. Dubinov, A. Satou, M. Ryzhii, V. Ryzhii, T. Otsuji. *Nanophotonics*, **7**, 741 (2018). DOI: 10.1515/nanoph-2017-0106
- [11] D.V. Fateev, K.V. Mashinsky, V.V. Popov. *Appl. Phys. Lett.*, **110**, 061106 (2017). DOI: 10.1063/1.4975829
- [12] I.S. Nefedov, C.A. Valaginnopoulos, L.A. Melnikov. *J. Opt.*, **15**, 114003 (2013). DOI: 10.1088/2040-8978/15/11/114003
- [13] O.N. Kozina, L.A. Melnikov. *Radiotekhnika i elektronika*, **67** (10), 1058 (2022) (in Russian). DOI: 10.31857/S0033849422100060
[O.N. Kozina, L.A. Melnikov. *J. Commun. Technol. Electron.*, **67** (10), 1304 (2022). DOI: 10.1134/S1064226922100060]
- [14] O.S. Kidwai, V. Zhukovsky, J.E. Sipe. *Phys. Rev. A*, **85**, 053842(12) (2012). DOI: 10.1103/PhysRevA.85.053842
- [15] A.A. Dubinov, V.Ya. Aleshkin, V. Mitin, T. Otsuji, V. Ryzhii. *J. Phys. Condens. Matter.*, **23**, 145302 (2011). DOI: 10.1088/0953-8984/23/14/145302
- [16] C. Virojanadara, M. Syväjärvi, R. Yakimova, L.I. Johansson, A.A. Zakharov, T. Balasubramanian. *Phys. Rev. B*, **78**, 245403 (2008). DOI: 10.1103/PhysRevB.78.245403
- [17] H. Mutschke, A.C. Andersen, D. Clement, Th. Henning, G. Peiter. *Astron. Astrophys.*, **345**, 87 (1999).
- [18] J. Chen, Z.H. Levine, J.W. Wilkins. *Phys. Rev. B*, **50** (16), 11514 (1994).
- [19] D.W. Berreman. *J. Opt. Soc. Am.*, **62**(4), 1157 (1972).
- [20] D.A. Yakovlev, V.G. Chigrinov. *Modeling and Optimization of the LCD Optical Performance* (Wiley, London, 2015)
- [21] S.P. Palto. *J. Experiment. Theor. Phys.*, **92** (4), 552 (2001). DOI: 10.1134/1.1371338
- [22] O.A. Golovanov, G.S. Makeeva, A.B. Rinkevich. *Tech. Phys.*, **61** (2), 274 (2016). DOI: 10.1134/S1063784216020122

Translated by A.Akhtyamov